

State preparation by optical pumping in erbium-doped solids using stimulated emission and spin mixing

B. Lauritzen,^{*} S. R. Hastings-Simon, H. de Riedmatten, M. Afzelius, and N. Gisin
Group of Applied Physics, University of Geneva, CH-1211 Geneva 4, Switzerland
 (Received 8 August 2008; published 6 October 2008)

Erbium-doped solids are potential candidates for the realization of a quantum memory for photons at telecommunication wavelengths. The implementation of quantum memory proposals in rare-earth-ion-doped solids require spectral tailoring of the inhomogeneous absorption profile by efficient population transfer between ground-state levels (spin polarization) using optical pumping. In this paper we investigate the limiting factors of efficient optical pumping between ground-state Zeeman levels in an erbium-doped Y_2SiO_5 crystal. We introduce two methods to overcome these limiting factors: stimulated emission using a second laser and spin mixing using radio frequency excitation. Both methods significantly improve the degree of spin polarization. Population transfer between two Zeeman levels with less than 10% of the total population in the initial ground state is achieved, corresponding to a spin polarization greater than 90%. In addition, we demonstrate spectral tailoring by isolating a narrow absorption peak within a large transparency window.

DOI: [10.1103/PhysRevA.78.043402](https://doi.org/10.1103/PhysRevA.78.043402)

PACS number(s): 32.80.Xx, 78.47.nd, 78.45.+h, 78.70.Gq

I. INTRODUCTION

In quantum-information applications based on optically addressed atoms or ions, it is often necessary to prepare these elements in specific hyperfine or Zeeman spin levels. Typically, this involves optical pumping from one ground-state spin level to another via an excited state. The preparation of the ions into a single well-defined state (spin polarization) is a required initial step for quantum memory protocols based on electromagnetically induced transparency [1–4], Raman interactions [5,6] and photon echoes using controlled reversible inhomogeneous broadening (CRIB) [7–10] or atomic frequency combs (AFCs) [11]. In particular, the implementation of these protocols in rare-earth (RE) ion-doped solids [12] requires spectral tailoring of the inhomogeneous absorption in order to isolate narrow absorption peaks.

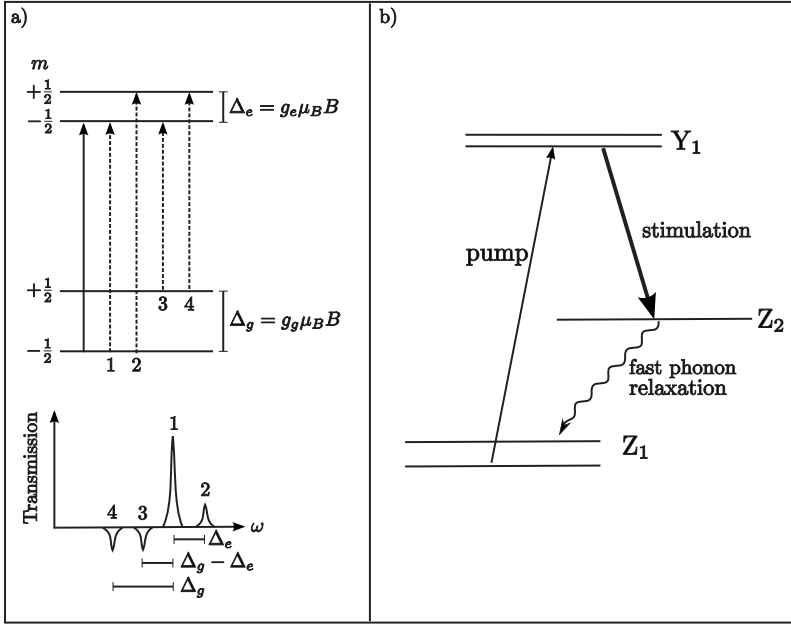
Among the various physical systems that have been considered for photonic quantum state storage, erbium-doped solids provide a unique system where a large number of stationary atoms can coherently absorb photons at the telecommunication wavelength of $1.53\ \mu\text{m}$. Quantum memories at telecommunication wavelengths are required for a range of efficient quantum repeater protocols [5,13,14]. In addition, erbium-doped solids have exceptional optical coherence properties. An optical coherence time as long as 6.4 ms has been measured in $\text{Er}^{3+}:\text{Y}_2\text{SiO}_5$ [15], which represents the longest optical coherence time measured in a solid. Another interesting property of Er^{3+} is that it is a Kramers ion with an odd number of electrons. This results in a large splitting between the ground-state levels via a first-order Zeeman interaction, which leads to a larger accessible frequency bandwidth for quantum memory applications. However, the unquenched electronic spin of Kramers ions results in strong spin-spin and spin-phonon interactions as compared to non-Kramers ions such as Pr and Eu. Therefore the ground-state population relaxation times are much shorter than in non-

Kramers ions, usually in the range of tens to hundreds of milliseconds [16,17]. In order to achieve a high degree of population transfer via optical pumping, it is necessary for the ground-state lifetime to be much longer than the excited-state lifetime. Achieving efficient population transfer in erbium-doped materials seems thus particularly challenging.

The spectroscopic properties of $\text{Er}^{3+}:\text{Y}_2\text{SiO}_5$ have been extensively studied, including optical coherence [15,18,19], spectral diffusion [19,20], hyperfine structure [21], Zeeman relaxation lifetimes [17], Zeeman g factors [22], and erbium-host interactions [23]. Slow light has also been achieved in this material using coherent population oscillation [24]. However, to our knowledge no study has been reported on the possibility of implementing efficient population transfer between the two Zeeman ground states to achieve a high degree of spin polarization.

In this paper, we investigate optical pumping between ground-state Zeeman levels of erbium ions doped into a Y_2SiO_5 crystal. We first observe the limitation of standard optical pumping. For $\text{Er}^{3+}:\text{Y}_2\text{SiO}_5$ an optical relaxation time of 11 ms [18] and a Zeeman relaxation lifetime of about 130 ms (at a magnetic field of 1.2 mT) [17] have been measured. The low ratio between these two relaxation lifetimes strongly limits the achievable population transfer efficiency. Another limiting factor is the branching ratio between the two optical transitions connecting the two ground-state Zeeman levels. We then show how an enhancement of the optical pumping efficiency can be achieved by decreasing the excited-state lifetime via optical stimulated emission and by improving spin branching ratios via radio frequency (rf) excitation. These techniques allow population transfer between the two Zeeman states with less than 10% of the total population remaining in the initial state, i.e., more than 90% spin polarization. We also demonstrate spectral tailoring in this crystal by preparing a narrow absorption line inside a wide transparency window (spectral pit), as required for the CRIB quantum memory scheme.

^{*}bjorn.lauritzen@physics.unige.ch



II. THEORY

Population transfer between the two closely spaced ground-state levels of a Λ system can be achieved by optical pumping via the excited-state level. In an optical pumping experiment, atoms are excited by a laser in resonance with the transition connecting one of the ground states to the excited state. The excited atoms can then decay into both ground states. Those that have decayed to the ground state that is not connected to the laser will in principle remain there for a time corresponding to the relaxation time between the ground states. If enough pumping cycles can be done within this time, the population from the initial ground state can be entirely transferred to the second ground state. The efficiency of this transfer is thus limited by the ratio of the excited-state lifetime (T_1) and the spin population lifetime of the ground-state levels (which we label T_Z , since in our case the ground-state levels are Zeeman levels) as well as the branching factor β . The latter is defined as the probability of the ion to relax into its initial state via spontaneous emission.

In materials with inhomogeneous broadening, population transfer by optical pumping is usually realized and investigated with spectral hole-burning techniques. In this scheme, the pump laser of frequency ω_0 [in resonance with transition 1, Fig. 1(a)] is focused on the sample for a duration T_{pump} , the burning time. Ions that are in resonance with ω_0 are transferred to the excited state. In order to probe the transmission, a weak pulse follows after a delay δt during which the frequency of the laser is scanned around ω_0 [see Fig. 2(b)]. The inhomogeneously broadened absorption shows a spectral hole at ω_0 which in general decays with the excited-state lifetime T_1 .

Some of the ions will, however, relax into the second ground-state Zeeman level. If the temperature is low enough ($T < 3$ K) such that Zeeman levels are thermally decoupled [17], the population of this level will then be increased and the absorption at $\omega = \omega_0 - (\Delta_g - \Delta_e)$ [transition 4 in Fig. 1(a)] will be enhanced. This enhancement is called a spectral an-

FIG. 1. (a) Spectral hole-burning spectrum of a four-level system. The laser is in resonance with the $-1/2 \rightarrow -1/2$ transition (solid line). The probe transitions (dashed lines) are labeled and the positions of the corresponding holes and antiholes in the transmission spectrum are shown below. The Zeeman splitting of the ground- and the excited-state levels, respectively, is given by $\Delta_{e,g} = \mu_B g_{e,g} B / \hbar$, where g_g and g_e are the g factors for the ground and the excited state, respectively, μ_B is the Bohr magneton, and B is the magnetic field. Note that, in addition to those shown in the figure, further holes and antiholes occur that are due to the inhomogeneous broadening of the absorption line [16,17,25]. (b) To enhance the efficiency of the population transfer the excited-state lifetime is artificially lowered by stimulated emission to the short-lived second Kramers doublet of the ground state (Z_2).

ti-hole. It will decay with the Zeeman lifetime T_Z . As long as the population in the two Zeeman levels has not relaxed to thermal equilibrium, a part of the spectral hole at ω_0 will persist. In case of a population transfer the hole should thus show two different decay times: T_1 from ions that decay from the excited back to the initial state and T_Z from ions that relax into the second Zeeman level. The occurrence of

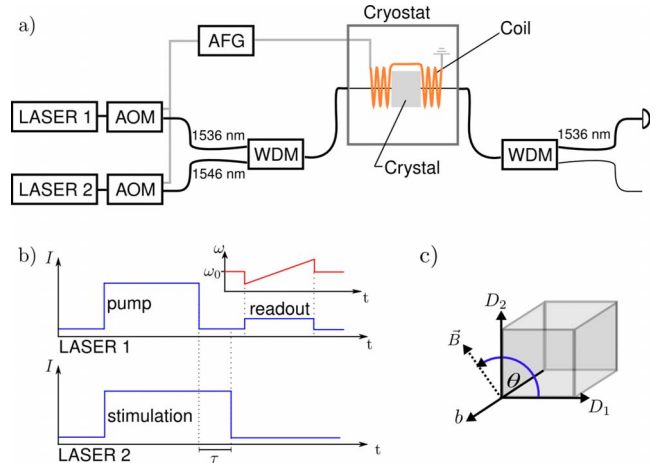


FIG. 2. (Color online) (a) Experimental setup. The laser for the hole burning ($\lambda = 1536$ nm) and the stimulation laser ($\lambda = 1546$ nm) could be intensity modulated independently with acousto-optic modulators (AOMs). They were coupled into the same fiber via a wave division multiplexer. The light of the stimulation laser was filtered out before detection using another WDM. A rf wave could be applied on the crystal using a coil in Helmholtz configuration which could be driven with an arbitrary function generator. (b) Typical pulse sequence. During the readout pulse the frequency of the pump laser was scanned in order to record the absorption profile. For measurement with stimulated emission, the stimulation laser is applied for a time $T_{\text{pump}} + \tau$, where τ can be varied. (c) Illustration of the angle of the magnetic field with respect to the crystal orientation.

the antihole and the long decay time (T_Z) for the central hole provide evidence of population transfer. Throughout this paper we speak of this method as the standard optical pumping scheme.

The intensity of the transmitted light is given by $I = I_0 \exp(-\alpha L)$, where I_0 is the intensity of the incident radiation and L the length of the sample. The absorption coefficient $\alpha = \sigma(N_2 - N_1)$, i.e., the logarithm of the transmitted intensity, gives rise to the relation between the number of ions $N_{1,2}$ in the ground and the excited states. σ is the cross section of the transition and can be considered as a constant. Since in this work the population rather than the measured intensities themselves is of interest, all curves that deal with quantities related to the absorption and transmission, respectively (such as the area or the depth of a spectral hole), are given with respect to the natural logarithm of the measured intensity.

To qualitatively understand the limiting factors in the population transfer process, one can use a simple rate equation model for a three-level Λ system. For the steady state in the case of standard optical pumping (see the Appendix) it is easy to derive that the ratio of populations in the ground states after optical pumping depends on the ratio between the Zeeman lifetime T_Z and the excited-state lifetime T_1 :

$$\frac{\rho_2}{\rho_1} = 1 + \frac{2T_Z}{T_1}, \quad (1)$$

where ρ_1 (ρ_2) is the population fraction in the initial (final) Zeeman state.

However, this holds only for the case in which all of the excited ions relax into the desired level. In RE-doped solids the selection rule for the electronic spin $\Delta m = 0$ normally is only slightly lifted by the crystal field and only a small part of the ions can be found in this decay channel. This motivates us to introduce an effective lifetime in the following manner:

$$T_{\text{eff}} = T_1 \frac{1}{1 - \beta}, \quad (2)$$

the branching factor $0 \leq \beta \leq 1$ being the probability that an ion will preserve its electron spin upon relaxation from the excited to the ground state. If β is low, the pump rate has to be accordingly high to transfer population into the excited state. On the other hand, a low branching factor is desirable if one wants the ions to relax into the second Zeeman level. The ratio between ions in either of the two ground-state levels is then given by $1 + 2T_Z/T_{\text{eff}}$ (see the Appendix).

In previous measurements on $\text{Er}^{3+}:\text{Y}_2\text{SiO}_5$, an excited-state lifetime of $T_1 = 11$ ms and a branching factor $\beta \geq 0.9$ were found [17]. This leads to an effective lifetime of $T_{\text{eff}} = 110$ ms which is of the same order as $T_Z \approx 130$ ms [17]. According to the model it is thus impossible to perform efficient population transfer between the Zeeman ground states of $\text{Er}^{3+}:\text{Y}_2\text{SiO}_5$ using standard optical pumping. However, by looking at Eqs. (1) and (2), one can devise methods to increase the efficiency of the population transfer. A first idea is to improve the lifetime ratio by artificially increasing the decay rate from the excited state. This can be achieved by

using stimulated emission to another short-lived ground-state level [see Fig. 1(b)] as proposed in [26]. The corresponding results are presented in Sec. IV B. Another possibility is to improve the branching ratio by mixing the spin level in the excited state using a radio frequency excitation. This technique is presented in Sec. IV C.

III. EXPERIMENTAL SETUP

The crystal, Y_2SiO_5 doped with Er^{3+} (10 ppm), belongs to the crystal space group C_{2h}^6 . The Er^{3+} ions replace Y^{3+} ions and occupy two crystallographic inequivalent sites of C_1 symmetry (sites 1 and 2) [18]. All measurements in this work were performed on ions at site 1. The relevant transition is from the $^4I_{15/2}$ to the $^4I_{13/2}$ level, which are split into eight (Z_i , $i=1, \dots, 8$, $i=1$ labeling the lowest crystal field level) and seven (Y_i , $i=1, \dots, 7$) Kramers doublets, respectively. All measurements were carried out on the $Z_1 \rightarrow Y_1$ transition having a wavelength of 1536 nm. Under a magnetic field each of the crystal field levels splits into two Zeeman levels ($m = \pm 1/2$).

The Y_2SiO_5 crystal has three mutually perpendicular optical-extinction axes labeled D_1 , D_2 , and b . The direction of light propagation is chosen parallel to the b axis. The crystal was cut along these axes and its dimensions were $3 \times 3.5 \times 4$ mm³ along b , D_1 , and D_2 , respectively. The magnetic field was applied in the D_1 - D_2 plane. In this case all ions of each site are magnetically equivalent [22]. The angle of the magnetic field is defined with respect to the D_1 axis [see Fig. 2(c)]. If not mentioned explicitly, all measurements were taken at an angle of $\theta = 135^\circ$, since here the transfer efficiency using standard optical pumping is higher [17].

The experimental setup is shown in Fig. 2(a). The crystal was placed on the cold finger of a liquid helium cryostat (Janis ST400) and could be cooled down to a temperature of about 2 K. All measurements, if not mentioned differently, were taken at 2.1 K. For optical pumping we used an external cavity diode laser (Toptica, $\lambda = 1536$ nm) which was operated in free-run mode and its jitter within the relevant time range was ≥ 1 MHz. For stimulated emission experiments a tunable diode laser (Nettest, $\lambda = 1546$ nm) was at our disposal. It was amplified with an erbium-doped fiber amplifier (EDFA) and could be tuned over a wide range. Both lasers could be gated independently using acousto-optical modulators (AOMs) and arbitrary function generators (AFGs). They were coupled into the same optical fiber via a wavelength division multiplexer (WDM). The light was focused into the crystal [diameter of focus (e^{-2}) ≈ 70 μm]. In order to avoid a large background in the detection due to fluorescence from the EDFA the stimulation laser was filtered out after passing the cryostat using a second WDM. The transmitted light was measured with a photodiode (NewFocus 2011). Furthermore, a Helmholtz coil placed around the crystal was at our disposal and could be used to apply rf pulses to the sample.

IV. EXPERIMENTS

A. Standard optical pumping

The first series of measurements was made with standard optical pumping (see Sec. II) in order to estimate the original

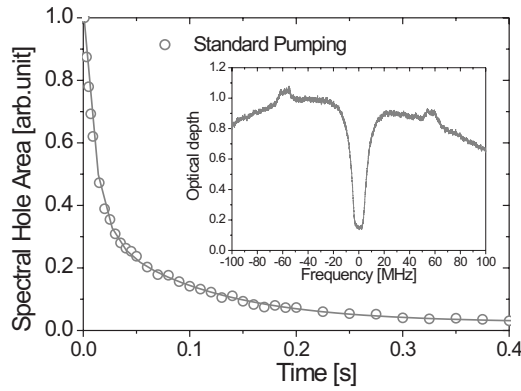


FIG. 3. Spectral hole area as a function of the readout delay time for the case of standard optical pumping. The decline is clearly dominated by the excited-state lifetime T_1 of 11 ms. The line is a fit to the data. Only a small fraction of the ions was transferred into the second Zeeman level and provides a slow component ($T_Z \approx 100$ ms) to the decline. The origin of the slowly decaying part is confirmed by the slight enhancement in the optical depth (antiholes) left and right of the wide spectral hole (pit) in the inset. The graph shows a zoom on the absorption line at about 2.8 ms after the burning pulse. Here the frequency of the pump laser was swept by 10 MHz during the burning pulse in order to widen the hole.

efficiency of the population transfer. A spectral hole was created by sending a resonant pump pulse of 200 ms into the crystal. The dynamics of the hole was then measured by probing it at different delays. The circles in Fig. 3 show the decay of the spectral hole using standard optical pumping. The dashed line is a fit to the data given by the sum of two exponential decays with rates of $1/T_1$ and $1/T_Z$, respectively.

The decay is clearly dominated by the excited-state lifetime $T_1 = 11$ ms. The contribution of the decay with T_Z is low which leads to the conclusion that only a very small fraction of the ions could be transferred to the second Zeeman level of Z_1 . This assumption is confirmed by the hole-burning spectrum shown in the inset of Fig. 3. For this measurement, a 10 MHz frequency sweep was applied to the pump laser, in order to widen the spectral hole. The enhancement of absorption at $\Delta_g - \Delta_e \approx \pm 60$ MHz (Fig. 1) is low, in contrast to what one would expect in the case of an efficient transfer of population. These observations show that the created spectral hole is mostly due to a storage of population in the excited state. Thus, as expected from the arguments given in Sec. II, optical pumping alone does not suffice to prepare the system into the required state.

B. Stimulated emission

A first possible solution to improve the optical pumping efficiency is to artificially increase the decay rate from the excited state by stimulating the emission to another short-lived ground-state level [see Fig. 1(b)] [26]. For this purpose, a second laser in resonance with the transition $Y_1 \rightarrow Z_2$ (1546 nm [18]) is applied simultaneously with the pump laser. Due to a strong coupling to phonon modes, mostly due to direct phonon emission, the excited crystal field levels (Z_2, Z_3, \dots) have nonradiative decay times in the range of

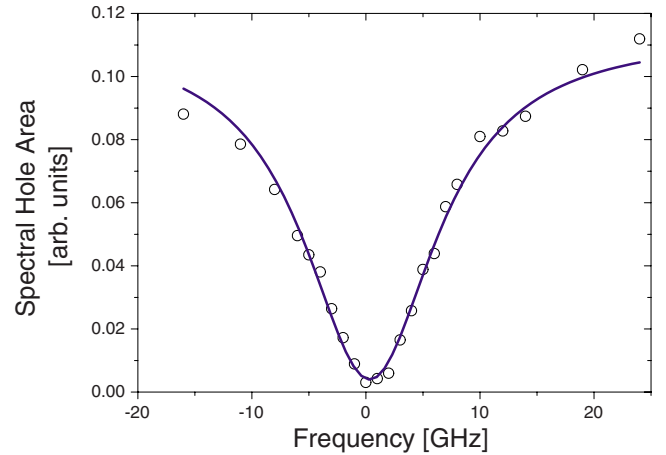


FIG. 4. (Color online) Spectral hole area as a function of the frequency of the stimulation laser at $T=4.1$ K. The burning time was 200 ms. The stimulation pulse was 1 ms longer than the burning pulse. The delay for the readout pulse was set to 2.5 ms. The solid line is a Lorentzian fit giving a full width at half maximum (FWHM) of 14 GHz.

nano- or picoseconds. Thus, population from these levels will immediately relax into ground state (Z_1).

We first characterize the stimulation process by measuring its dependence on the frequency of the stimulation laser. Since the homogeneous broadening of the transition is expected to be larger than the inhomogeneous broadening [27], due to the short nonradiative decay times, this gives a direct measure of the homogeneous linewidth. It has been done by measuring the size of the spectral hole as a function of the frequency of the stimulation laser at 4.1 K. At this temperature the ground-state Zeeman levels are thermally coupled [17] and therefore only ions in the excited state (i.e., ions that have not been stimulated down) contribute to the hole. The results are shown in Fig. 4. For this measurement, the stimulation pulse was 1 ms longer than the pump pulse. We see that, when the stimulation laser is in resonance, the spectral hole almost completely vanishes, which shows that one can efficiently empty the excited state using this method. We find the linewidth to be about 14 GHz, which corresponds to a lifetime in the picosecond range. This is nine orders of magnitude shorter than the Zeeman lifetime and confirms that the Z_2 level is suitable for the application described above.

Another quantity of interest is the rate at which stimulation laser moves the ions down from the excited to the ground state (Z_2). To measure this quantity a pump pulse with $T_{\text{pump}} = 100$ ms was sent into the sample. The crystal temperature was chosen to be 4.3 K so that also in this case the size of the hole would be given only by the fraction of ions that remained in the excited state. Simultaneously with the pump pulse, a stimulation pulse with a duration $T_{\text{pump}} + \tau$ was applied [see Fig. 2(b)]. The size of the remaining hole as a function of τ was recorded and the data were fitted with an exponential decay of which the stimulation rate could be extracted. The inset of Fig. 5 shows these data for three different values of applied stimulation power. Each of the lines is a fit to the respective data. Note that there is an

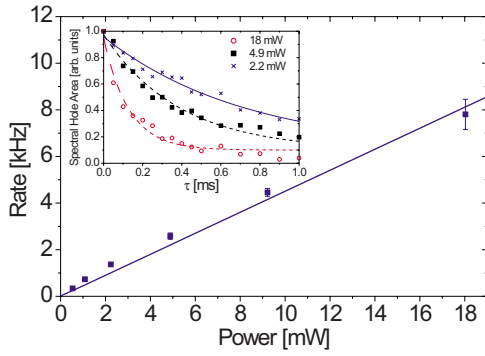


FIG. 5. (Color online) Stimulation rate on the $Y_1 \rightarrow Z_2$ transition vs applied laser power. The rate at which ions are stimulated down grows linearly with the power of the stimulation laser. It was extracted from the decay curves shown in the inset and as described in the text. Curves for three different values of the power of the stimulation laser are shown. Each data set is normalized to its maximum value ($\tau=0$). The offset of 0.1 is due to persistent holes, which have already been observed and discussed in [17].

offset, which has its origin in long-lived holes that occur even at this temperature for a small subset of ions [17]. It was set to be the same for all curves. The stimulation rate as a function of the stimulation power is plotted in Fig. 5. As one would expect the stimulation rate increases linearly with power. For this measurement, the maximal power of the stimulation laser on the sample was 20 mW and it was limited by the maximal output power of the EDFA. The measurements were taken with a magnetic field of 27.4 mT at an angle of $\theta=30^\circ$ with the D_1 axis. The average beam diameter (e^{-2}) in the crystal was $83 \mu\text{m}$.

Let us now investigate the effect of stimulated emission on the population transfer by optical pumping. In Fig. 6 one can see that the application of the stimulation laser simultaneously with the pump laser indeed leads to a significant enhancement of the transfer efficiency. The decay of the spectral hole at a temperature of 2.1 K is shown for the case of standard optical pumping (open circles) and optical pumping assisted by stimulated emission (plain triangles). For standard optical pumping, the decay is dominated by the time constant $T_1=11$ ms as explained in Sec. IV A. In contrast, the decay for the stimulated optical pumping is dominated by a slower decay time, which corresponds to $T_Z \approx 100$ ms. This indicates that a significant part of the population is now transferred to the other Zeeman level by the optical pumping process.

This hypothesis is confirmed by directly measuring the residual absorption after the optical pumping, as shown in the inset of Fig. 6. In order to obtain a reference for the transmission out of resonance, the entire inhomogeneously broadened absorption line was measured (only a zoom is shown). A spectral pit was created using stimulated optical pumping by sweeping the frequency of the pump laser over a range of 10 MHz while burning. For this measurement, the stimulation pulse was 1 ms longer than the pump pulse in order to deexcite population remaining in the excited state to the ground state. Therefore the transparency in the central pit is mostly due to ions transferred to the other ground state. The optical depth without optical pumping is $\alpha L_0=1$, while

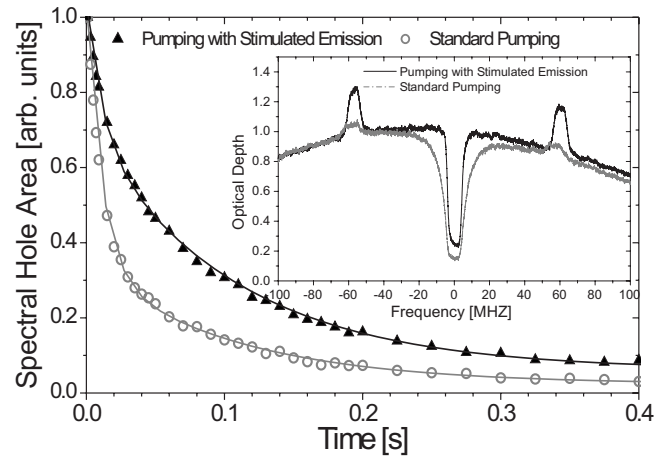


FIG. 6. Spectral hole area as a function of the readout delay time with (triangles) and without (open circles) stimulated emission. In the case in which the stimulation laser is applied a clearly enhanced contribution from ions transferred to the second Zeeman level can be observed. The corresponding hole decays with $T_Z \approx 100$ ms and the overall decay shows a much stronger contribution of this slow component than it can be observed for standard optical pumping. The enhancement in population transfer is confirmed by the strong antihole shown in the inset. The figure shows the absorption at about 2.8 ± 0.3 ms after the burning pulse. For this measurement, a 10 MHz sweep was applied on the pump laser, the stimulation pulse was 1 ms longer than the pump pulse, and the stimulation power in front of the cryostat was 50 mW.

the residual optical depth after population transfer is $\alpha L_{\text{res}} \approx 0.25$. The enhanced absorption which occurs in the form of wide antihole on both sides of the pit confirms, as explained in Sec. II, that the population was transferred as intended. From this measurement, it is possible to estimate the efficiency of the population transfer. The fraction of ions remaining in the initial Zeeman state $\rho_{1,\text{res}}$ can be estimated by $\rho_{1,\text{res}} = \alpha L_{\text{res}} / \alpha L_0 \approx 0.25$. Since initially the two Zeeman states are equally populated, this means that 12.5% of the total number of atoms is remaining in the initial state, within the frequency range optically pumped. If one assumes that all atoms that are not in the initial state have been transferred to the other Zeeman level, one can compute the ratio $\rho_2 / \rho_1 = 7$. This is much lower than would be expected from the simple model presented in Sec. II (see also Appendix). This shows that, while the model presented helps to understand the process of optical pumping, it is too simplified to give quantitative estimations.

C. Spin mixing

Although stimulated optical pumping greatly increases the population transfer efficiency, the fraction of ions remaining in the initial ground state is still high. This is in part due to the high value of the branching factor β for this transition. In Ref. [17], β was estimated to be larger than 0.9 for a magnetic field applied at $\theta=135^\circ$ [see Fig. 2(c)], from comparison between experimental data and numerical simulations. This means that the spin is conserved to a high degree during the decay from the excited state. From the measurement of

the last section, this seems to hold even for decay through the the state Z_2 , which involves phononic relaxation. In this section, we present a technique to improve the branching ratio for optical pumping applications.

An idea to overcome this problem in general is to artificially change the spin by mixing the population of the two Zeeman levels of the excited state using rf excitation. For this purpose a pair of Helmholtz coils¹ was placed around the crystal [see Fig. 2(a)]. Note that a difference of the g factors for the ground and the excited states is necessary in order not to mix the spin population of the ground state levels as well. In $\text{Er}^{3+}:\text{Y}_2\text{SiO}_5$ $g_g=12$ and $g_e=8$ [for \vec{B} at an angle of $\theta=135^\circ$; see Fig. 2(c)] [22]. For electronic spins with such large g factors, the magnetic dipole moment of the spin transition is large ($\mu=112$ MHz/mT), so that significant mixing can be obtained with moderate rf power. The rf pulse was applied simultaneously with the pump pulse (duration 200 ms). A 1- μs -long linear frequency sweep was continuously repeated during the burning process. Due to the inhomogeneity of the external magnetic field the bandwidth, i.e., the size of the sweep, had to be chosen high (10–20 MHz). The required central frequency corresponds to Δ_e in Fig. 1 and could be extracted from a hole-burning spectrum.

The effect of the rf mixing was measured by estimating the fraction of atoms remaining in the initial state after optical pumping, similarly to the measurement made in Sec. IV B. For this measurement however, both stimulated emission and rf excitation were applied. Figure 7 shows the fraction of the total number of atoms remaining in the initial state as a function of the rf voltage. A significant enhancement of the transfer due to the rf wave can be observed. This enhancement, however, is quickly saturated when the rf power is increased. This might be explained by the achievement of an equilibrium between the populations of the two Zeeman levels. The inset of Fig. 7 shows a zoom of the spectral pit created with and without rf mixing. For this measurement, the number of atoms in the initial state was 8%, as compared to 12.5% without rf mixing applied (Sec. IV B). Hence, a spin polarization of 92% within the optically pumped bandwidth has been achieved.

D. Spectral tailoring

The ability to tailor the absorption profile is important for quantum memory proposals such as CRIB or AFC, as well as proposals for quantum logic gates in RE-doped solids [28]. To illustrate this capacity in $\text{Er}^{3+}:\text{Y}_2\text{SiO}_5$, we isolated a narrow absorption line within a large transparency window (spectral pit), with the help of the two methods presented above. For this purpose, we used a simple technique consisting of sweeping the laser frequency during the 200-ms-long pump pulse and gating off the pump laser for a short time at the center of the frequency sweep. The total frequency range was swept in 100 μs , resulting in 2000 frequency sweeps.

¹The dimensions of the coil used for the spin-mixing experiments were diameter = 4 mm, length of each coil ≈ 3 mm, distance between coils ≈ 3 mm, three turns on each side. The central axis was parallel to the axis of light propagation.

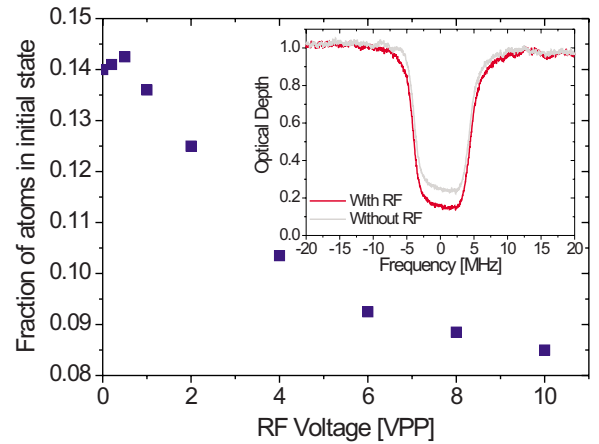


FIG. 7. (Color online) Efficiency of the spin-mixing method as a function of the applied rf voltage. The central frequency of the rf wave is 135 MHz, corresponding to the splitting of the excited-state Zeeman levels. The efficiency is estimated by measuring the fraction of the total number of atoms remaining in the initial state after optical pumping. Both stimulated emission (50 mW) and rf mixing are used. The duration of the pump sequence is 200 ms. The stimulation pulse is 1 ms longer than the pump pulse, in order to empty the excited state. The inset shows an example of a spectral pit created by population transfer with a frequency sweep of 10 MHz, without and with rf mixing (with the highest rf voltage of 10 V peak to peak).

An example of spectral tailoring is shown in Fig. 8. The width of the pit is 50 MHz while the absorption width of the peak at the center of the pit is 2 MHz. This is much broader than the homogeneous linewidth of the transition [18]. The width of the peak is likely to be limited by the linewidth of our free-running laser, which is larger than 1 MHz for the time scale of the burning pulse. The fact that we sweep the laser frequency by scanning the laser current might also de-

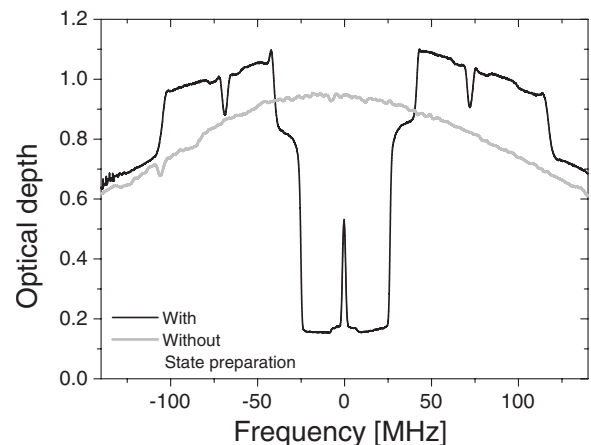


FIG. 8. Spectral tailoring in $\text{Er}^{3+}:\text{Y}_2\text{SiO}_5$ (black curve). A narrow absorption line (FWHM 2 MHz) could be established inside a spectral pit (FWHM 50 MHz). An interesting feature is that the structure written into the absorption can as well be observed in the corresponding antihole, which again confirms the population transfer into the second Zeeman level of the ground state. The gray curve corresponds to the inhomogeneous absorption without the state preparation sequence. For further details, see text.

grade the linewidth. Stabilizing the laser frequency will be required in order to obtain narrower absorption peaks. Furthermore, the use of more sophisticated hole-burning techniques will also be needed [28–32] in order to achieve an absorption width in the kilohertz range. In this limit one would also have to consider the broadening of the homogeneous line due to the artificially lowered excited-state lifetime induced by the stimulation laser. A possibility to solve this problem would be to excite ions and stimulate them down sequentially.

Although the methods developed in this paper allow a significant improvement of population transfer efficiency as compared to standard optical pumping, there is still a residual absorption in the spectral pit. This will act as a passive loss for light storage protocols. Further efforts will thus be needed in order to optimize light storage efficiency. Note, however, that the width of the spectral pit (50 MHz) is much larger than can be achieved in non-Kramers ions that have been used for such purposes so far, such as praseodymium [10,32] or europium [29,33]. This shows the potential of Er-doped solids for obtaining large frequency bandwidths for quantum storage applications.

V. CONCLUSIONS

Erbium-doped solids are promising candidates for the implementation of quantum memories at telecommunication wavelengths. We have shown and discussed the difficulties for state preparation by optical pumping in $\text{Er}^{3+}:\text{Y}_2\text{SiO}_5$, including the ratio between the excited-state and the Zeeman lifetimes and the branching factor β . With stimulated-emission-assisted optical pumping and spin mixing using rf excitations, we have investigated two methods to alleviate these problems. We have shown that their application indeed leads to a significant enhancement of the optical pumping efficiency. Population transfer between two Zeeman levels with less than 10% of the total population in the initial level has been demonstrated. This corresponds to a spin polarization of 90%. Note that the techniques used here can also be applied to other RE-doped solids. In particular, it might be useful to enhance optical pumping efficiency in other Kramers ions, such as neodymium [16].

Further improvements might be obtained by increasing stimulation rates with higher laser powers and using coherent rf population transfer between the two excited states. Another possibility for improving the branching ratio could be to apply the magnetic field at particular angles where the spin conservation selection rule is relaxed [25,34,35]. In order to increase the population lifetime of Zeeman levels, it might be interesting to work at higher magnetic field (hundreds of millitorrs), in order to reduce spin-spin interactions. Other crystals might also be explored, e.g., Y_2O_3 , to search for longer Zeeman lifetimes. Finally, it would also be interesting to investigate hyperfine states, which might have longer spin-population relaxation lifetimes [21].

We also demonstrated spectral tailoring in $\text{Er}^{3+}:\text{Y}_2\text{SiO}_5$ by isolating a narrow absorption peak within a wide transparency window, as required for the CRIB quantum memory scheme. Although further progress remains to be made to

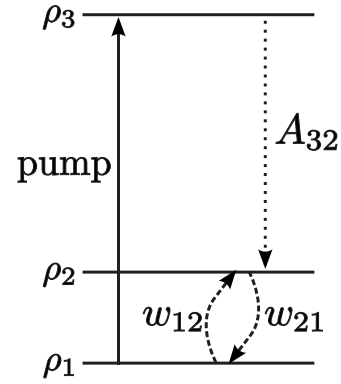


FIG. 9. Level scheme to estimate the population ratio in the case of standard optical pumping.

improve the population transfer efficiency with higher optical depth, the achievement of spectral tailoring in erbium-doped solids will allow proof of principle experiments of light storage with quantum memory protocols. Hence, with this work a further step toward a solid-state-based quantum memory at telecommunication wavelength has been accomplished.

ACKNOWLEDGMENTS

We would like to thank Marko Lovric and Roman Kolesov for their advice concerning the design of the rf setup. Furthermore, we would like to thank the group of Professor D. van der Marel, Mehdi Brandt, J. van Mechelen, and Violeta Guritanu for experimental assistance, as well as Professor M. Chergui (EPFL) for loaning us the cryostat. Technical support by C. Barreiro and J. D. Gauthier is acknowledged. This work was supported by the Swiss NCCR Quantum Photonics and the European Commission under the Integrated Project Qubit Applications (QAP) funded by the IST directorate.

APPENDIX: LIFETIME RATIO

1. Standard optical pumping

The low efficiency of the population transfer was ascribed to the ratio between the excited state lifetime T_1 and the ground-state Zeeman lifetime T_Z as well as the branching factor β . The corresponding formulas [Eqs. (1) and (2), Sec. II] were found using the following simple rate equation model.

Let ρ_1 , ρ_2 and ρ_3 be the population fraction in the two ground states and in the excited state, respectively, as shown in Fig. 9. The laser is in resonance with the transition between levels 1 and 3. For the population of the second Zeeman ground-state level the population dynamics is given by

$$\frac{d}{dt}\rho_2 = w_{12}\rho_1 - w_{21}\rho_2 + A_{32}\rho_3. \quad (\text{A1})$$

A_{32} is the Einstein coefficient for spontaneous emission and w_{12} and w_{21} are the spin-lattice relaxation rates. In the case

considered by Gorju *et al.* [26], a term that corresponds to w_{12} does not occur since the target state is a crystal field level and the relevant phonon decay is a one-way process. However, the calculations are still quite similar. In the steady state,

$$\frac{d}{dt}\rho_2 = 0, \quad (\text{A2})$$

and

$$\rho_1 = \rho_3, \quad (\text{A3})$$

where the second equality holds for the case of sufficiently high pump power, i.e., a saturation of the considered transition. If we further assume $w_{12}=w_{21}$, which is a good approximation since the thermal energy $k_B T$ is much larger than the splitting between the two levels, it follows from Eq. (A1) that the ratio between the number of ions in either of the lower states is given by

$$\frac{\rho_2}{\rho_1} = 1 + \frac{A_{32}}{w_{12}} = 1 + \frac{2T_Z}{T_1}. \quad (\text{A4})$$

The factor 2 in the numerator of the lifetime ratio occurs since $T_Z = 1/(w_{12}+w_{21}) = 1/(2w_{12})$ [36].

So far, it is assumed that all ions decay into the second Zeeman level. In this case $1/A_{32}=T_1$. However, one has to take into account that only a fraction of the ions in the excited state will do so. Supposing that the excited-state lifetime is given by $T_1 = 1/A$ with $A = A_{31} + A_{32}$ and with the defi-

nition of the branching factor $\beta = A_{31}/(A_{31} + A_{32})$ [which gives $1 - \beta = A_{32}/(A_{31} + A_{32})$] we can define the effective lifetime

$$T_{\text{eff}} = \frac{1}{A_{32}} = \frac{T_1}{1 - \beta}. \quad (\text{A5})$$

Plugging this into Eq. (A4), we get

$$\frac{\rho_2}{\rho_1} = 1 + \frac{2T_Z}{T_{\text{eff}}}. \quad (\text{A6})$$

2. Stimulated emission

In the case of stimulated emission as presented in Sec. IV B, the spontaneous emission rate A has to be replaced with the stimulation rate Γ . Due to its extremely low lifetime, the role of the level Z_2 (Fig. 1) can be neglected. According to Eq. (A6), the population ratio is now given by

$$\frac{\rho_2}{\rho_1} = 1 + 2(1 - \beta)\Gamma T_Z. \quad (\text{A7})$$

If one considers a branching factor $\beta = 0.95$ and a stimulation rate of $\Gamma = 7$ kHz, with a Zeeman lifetime of 100 ms we compute a ratio of 71, which is significantly higher (\sim one order of magnitude) than found in the experiment. This can be explained by the fact that the model is extremely simplified as compared to reality. Among other factors, the role of other decay channels and the possibility of a different branching factor for a decay from the Z_2 level could not be taken into account. Nevertheless, this model can help us to understand qualitatively the processes of optical pumping in the system.

-
- [1] M. Fleischhauer and M. D. Lukin, *Phys. Rev. Lett.* **84**, 5094 (2000).
- [2] J. J. Longdell, E. Fraval, M. J. Sellars, and N. B. Manson, *Phys. Rev. Lett.* **95**, 063601 (2005).
- [3] M. D. Eisaman, A. André, F. Massou, M. Fleischhauer, A. S. Zibrov, and M. D. Lukin, *Nature (London)* **438**, 837 (2005).
- [4] T. Chanelière, D. N. Matsukevich, S. D. Jenkins, S.-Y. Lan, T. A. B. Kennedy, and A. Kuzmich, *Nature (London)* **438**, 833 (2005).
- [5] L.-M. Duan, M. D. Lukin, J. I. Cirac, and P. Zoller, *Nature (London)* **414**, 413 (2001).
- [6] J. Nunn, I. A. Walmsley, M. G. Raymer, K. Surmacz, F. C. Waldermann, Z. Wang, and D. Jaksch, *Phys. Rev. A* **75**, 011401(R) (2007).
- [7] S. A. Moiseev and S. Kröll, *Phys. Rev. Lett.* **87**, 173601 (2001).
- [8] M. Nilsson and S. Kröll, *Opt. Commun.* **247**, 393 (2005).
- [9] B. Kraus, W. Tittel, N. Gisin, M. Nilsson, S. Kröll, and J. I. Cirac, *Phys. Rev. A* **73**, 020302(R) (2006).
- [10] G. Hétet, J. J. Longdell, A. L. Alexander, P. K. Lam, and M. J. Sellars, *Phys. Rev. Lett.* **100**, 023601 (2008).
- [11] M. Afzelius, C. Simon, H. de Riedmatten, and N. Gisin, e-print arXiv:0805.4164.
- [12] R. M. Macfarlane, *J. Lumin.* **100**, 1 (2002).
- [13] N. Sangouard, C. Simon, J. Minář, H. Zbinden, H. de Riedmatten, and Nicolas Gisin, *Phys. Rev. A* **76**, 050301(R) (2007).
- [14] N. Sangouard, C. Simon, B. Zhao, Y.-A. Chen, H. de Riedmatten, J.-W. Pan, and N. Gisin, *Phys. Rev. A* **77**, 062301 (2008).
- [15] Y. Sun, C. W. Thiel, R. L. Cone, R. W. Equall, and R. L. Hutcheson, *J. Lumin.* **98**, 281 (2002).
- [16] S. R. Hastings-Simon, M. Afzelius, J. Minář, M. U. Staudt, B. Lauritzen, H. de Riedmatten, N. Gisin, A. Amari, A. Walther, S. Kröll, E. Cavalli, and M. Bettinelli, *Phys. Rev. B* **77**, 125111 (2008).
- [17] S. R. Hastings-Simon, B. Lauritzen, M. U. Staudt, J. L. M. van Mechelen, C. Simon, H. de Riedmatten, M. Afzelius, and N. Gisin, *Phys. Rev. B* **78**, 085410 (2008).
- [18] Thomas Böttger, C. W. Thiel, Y. Sun, and R. L. Cone, *Phys. Rev. B* **74**, 075107 (2006).
- [19] Thomas Böttger, C. W. Thiel, Y. Sun, and R. L. Cone, *Phys. Rev. B* **73**, 075101 (2006).
- [20] V. Crozatier, G. Gorju, F. Bretenaker, J.-L. Le Gouët, I. Lorgère, O. Guillot-Noël, and P. Goldner, *J. Lumin.* **127**, 65 (2007).
- [21] O. Guillot-Noël, Ph. Goldner, Y. L. Du, E. Baldit, P. Monnier, and K. Bencheikh, *Phys. Rev. B* **74**, 214409 (2006).
- [22] Y. Sun, T. Böttger, C. W. Thiel, and R. L. Cone, *Phys. Rev. B*

- 77, 085124 (2008).
- [23] O. Guillot-Noel, H. Vezin, Ph. Goldner, F. Beaudoux, J. Vincent, J. Lejay, and I. Lorgeré, *Phys. Rev. B* **76**, 180408(R), (2007).
- [24] E. Baldit, K. Bencheikh, P. Monnier, J. A. Levenson, and V. Rouget, *Phys. Rev. Lett.* **95**, 143601 (2005).
- [25] A. Louchet, J. S. Habib, V. Crozatier, I. Lorgere, F. Goldfarb, F. Bretenaker, J.-L. Le Gouët, O. Guillot-Noël, and Ph. Goldner, *Phys. Rev. B* **75**, 035131 (2007).
- [26] G. Gorju, A. Louchet, D. Paboef, F. Bretenaker, F. Goldfarb, T. Chanelière, I. Lorgeré, J.-L. Le Goët, O. Guillot-Noël, and P. Goldner, *J. Phys.: Condens. Matter* **19**, 386226 (2007).
- [27] E. Dusrvire, *Erbium Doped Fiber Amplifiers* (Wiley, New York, 1994), pp.215–2225.
- [28] L. Rippe, M. Nilsson, S. Kröll, R. Klieber, and D. Suter, *Phys. Rev. A* **71**, 062328 (2005).
- [29] G. J. Pryde, M. J. Sellars, and N. B. Manson, *Phys. Rev. Lett.* **84**, 1152 (2000).
- [30] M. J. Sellars, G. J. Pryde, N. B. Manson, and E. R. Krausz, *J. Lumin.* **87-89**, 833 (2000).
- [31] F. de Seze, V. Lavielle, I. Lorgeré, and J. L. Le Gouët, *Opt. Commun.* **223**, 321 (2003).
- [32] M. Nilsson, L. Rippe, S. Kröll, R. Klieber, and D. Suter, *Phys. Rev. B* **70**, 214116 (2004).
- [33] M. Nilsson, L. Rippe, N. Ohlsson, T. Christiansson, and S. Kröll, *Phys. Scr., T* **102**, 178 (2002).
- [34] F. de Seze, A. Louchet, V. Crozatier, I. Lorgeré, F. Bretenaker, J.-L. Le Gouët, O. Guillot-Noël, and P. Goldner, *Phys. Rev. B* **73**, 085112 (2006).
- [35] C. Thiel (private communication).
- [36] *Electron Paramagnetic Resonance*, edited by S. Geschwind (Plenum Press, New York, 1972).